



**HAL**  
open science

## Investigation and properties of novel low melting glasses in the ternary system $\text{Sb}_2\text{O}_3\text{-PbO-Me}_2\text{O}_3$

Yasmina Taibi, Marcel Poulain, Messaoud Legouera, Alima Mebrek

### ► To cite this version:

Yasmina Taibi, Marcel Poulain, Messaoud Legouera, Alima Mebrek. Investigation and properties of novel low melting glasses in the ternary system  $\text{Sb}_2\text{O}_3\text{-PbO-Me}_2\text{O}_3$ . *International Journal of Applied Glass Science*, 2022, 13 (2), pp.254-262. 10.1111/ijag.16545 . hal-03516407

**HAL Id: hal-03516407**

**<https://hal.science/hal-03516407>**

Submitted on 25 Aug 2022

**HAL** is a multi-disciplinary open access archive for the deposit and dissemination of scientific research documents, whether they are published or not. The documents may come from teaching and research institutions in France or abroad, or from public or private research centers.

L'archive ouverte pluridisciplinaire **HAL**, est destinée au dépôt et à la diffusion de documents scientifiques de niveau recherche, publiés ou non, émanant des établissements d'enseignement et de recherche français ou étrangers, des laboratoires publics ou privés.

# INVESTIGATION AND PROPERTIES OF NOVEL LOW MELTING GLASSES IN THE TERNARY SYSTEM $\text{Sb}_2\text{O}_3\text{-PbO-Me}_2\text{O}_3$

Y. Taibi<sup>a</sup>, M. Poulain<sup>b</sup>, M. Legouera<sup>c</sup>, A. Mebrek<sup>d</sup>

<sup>a</sup> Laboratoire de Mines, Métallurgie et Matériaux, ENSMM-Annaba, Ex CEFOS-Sidi Amar, 2300 Annaba, Algérie

<sup>b</sup> Sciences Chimiques, Université de Rennes 1, Campus Beaulieu, F-35042 Rennes, France

<sup>c</sup> Dept Mécanique, Université de Skikda, 21000 Algérie

<sup>d</sup> Research Center in Industrial Technology CRTI, P.O. Box 64, Cheraga 16014, Algiers, Algeria

## Abstract

New glasses based on  $\text{Sb}_2\text{O}_3\text{-PbO}$  association have been synthesized and characterized. The limits for glass formation have been investigated in ternary systems encompassing an oxide of IIIA group elements like  $\text{Al}_2\text{O}_3$ ,  $\text{Ga}_2\text{O}_3$  and  $\text{In}_2\text{O}_3$  as the third component. Fast quenching is required to prevent melt crystallization, which results in thin samples. Chemical analysis of elements shows a rather good agreement between nominal and analyzed compositions. Glass transition temperature,  $T_g$ , ranges between  $255^\circ\text{C}$  and  $280^\circ\text{C}$ , depending on composition. Density and hardness have been measured for typical composition.

## Keywords

Lead antimony glass. Thermal properties. Density. Hardness

## 1. Introduction

The use of lead oxide as a significant glass component is older than modern chemistry and physics. In 1675 George Ravenscroft defined a new glass composition containing lead oxide, leading to larger working range in the molten state, reduced hardness and higher refractive index, which increases surface brightness [1, 2].

Heavy Metal Oxide Glasses (HMOG) make a family of special glasses that has been the subject of numerous studies. They may be roughly defined as glasses free of classical vitrifiers  $\text{SiO}_2$ ,  $\text{B}_2\text{O}_3$ ,  $\text{P}_2\text{O}_5$  [3]. These glasses exhibit high refractive index, close to 2, large optical non-linearity and extended optical transmission in the infrared spectrum [4, 5, 6]. Among HMOG, germanate glasses appear as an intermediate group as  $\text{GeO}_2$  is considered as a classical network former according to Zachariasen's rules [7], and also because their refractive index is somewhat lower.

1 Antimonite glasses based on  $\text{Sb}_2\text{O}_3$  have attracted growing interest, mainly because numerous  
2 glass forming systems have been identified so far, especially in polyanionic systems:  
3 oxyhalides and oxysulfides. In addition their stability against devitrification may be very  
4 large. Antimony oxide glasses have been reported in association to alkali oxides and in  
5 multicomponent systems [8, 9, 10].  
6

7 According to previous reports,  $\text{PbO-Sb}_2\text{O}_3$  glasses exhibit good chemical durability and low  
8 crystallization rates [11, 12]. Addition of the oxides of III A group elements like  $\text{Al}_2\text{O}_3$ ,  
9  $\text{Ga}_2\text{O}_3$  and  $\text{In}_2\text{O}_3$  to the  $\text{PbO-Sb}_2\text{O}_3$  based glass is likely to ameliorate their physical  
10 properties. The choice of these oxides was based on the occurrence of a binary glass forming  
11 range in combination to  $\text{PbO}$ . Table 1 reports the compositional limits of these binary glasses:  
12  
13

14 Table 1  
15

$\text{M}_2\text{O}_3$	Maximum reported glass forming range (mol % $\text{PbO}$ )
$\text{Al}_2\text{O}_3$	50-95 mol% $\text{PbO}$ [13]; 67 – 95 mol% $\text{PbO}$ [14]
$\text{Ga}_2\text{O}_3$	69 -81mol% $\text{PbO}$ [15]; 58 -82 mol% $\text{PbO}$ [16]; 57 - 82 mol% $\text{PbO}$ [17];
$\text{In}_2\text{O}_3$	< 5 mol% $\text{PbO}$ [18]

16  
17  
18  
19  
20  
21

22 The aim of the present work is to explore new glass compositions in multicomponent systems  
23 based on antimony oxide and to assess the potential of these glasses  
24  
25

## 26 2. Experimental 27

28 Materials used in this research are  $\text{Sb}_2\text{O}_3$  (99,9%),  $\text{PbO}$  (99,9%),  $\text{In}_2\text{O}_3$  (98%),  $\text{Ga}_2\text{O}_3$  (98%),  
29 and  $\text{Al}_2\text{O}_3$  (98%) from Aldrich, WWR and Metal Europe. Glass samples were prepared using  
30 the standard melt-quenching technique. Crystalline powders were intimately mixed in an  
31 agate mortar. Then batch was heated up to melting in glass crucible for 5 min. Finally the  
32 melts were cast and quenched between two brass plates to obtain a fast cooling rate close to a  
33 few hundred K/S. In these conditions, sample thickness ranges between 0.8 and 1mm.  
34  
35

36 Main physical characterizations include X ray diffraction, thermal analysis microhardness and  
37 density. X-ray diffraction patterns were obtained using  $\text{Cu K}\alpha$  radiation on Philips PW1830  
38 diffractometer. Differential scanning calorimetric measurements were performed on small  
39 samples using a DSC 2010 from TA Instrument in aluminum sealed pans under  $\text{N}_2$   
40 atmosphere. Current heating rate was  $10 \text{ K}\cdot\text{min}^{-1}$  and experimental error was  $\pm 2^\circ\text{C}$  for glass  
41 transition and onset of crystallization. Chemical composition was checked using Oxford Link  
42 ISIS probe in a JEOL 6400 Scanning Electron Microscope dispersive  $\gamma$ -ray spectrometer  
43 working at 20 KV. Density was measured using an ACCUPYC 1330 Micrometrics Helium  
44 Picnometer with a precision of about  $\pm 0,0005\text{g}/\text{cm}^3$ . The samples were indented with  
45 Matsuzawa MXT set-up. The value is averaged from 10 indentations or more, made on each  
46 sample.  
47  
48  
49  
50

## 51 3. Results 52

### 53 3.1 Glass formation: 54

55 Our primary investigation of the binary  $\text{Sb}_2\text{O}_3$ - $\text{PbO}$  based system confirms that the limits for  
56 glass formation are extended, when faster quenching rates are used. These limits lie between  
57 80 and 10% mol  $\text{Sb}_2\text{O}_3$  as shown in Fig1.  
58  
59  
60  
61  
62  
63  
64  
65

Prepared glasses are stable at room atmosphere. At visual inspection, they appear transparent and yellow colored for glass samples between 80 and 40 mol %  $\text{Sb}_2\text{O}_3$ . As PbO content increases, glass samples appear dark. This coloration arises from lead reduction: Indeed, as shown in figure 2, a metallic phase area corresponding to pure lead was observed in a dark glass sample. In practice, melt must be kept at room atmosphere for a longer time –e.g. 8 mn– to ensure oxidizing atmosphere.

In order to confirm glass composition, elemental analysis was performed for some samples with nominal composition  $(100-x) \text{Sb}_2\text{O}_3.x\text{PbO}$  ( $x= 50,60,70,80,90$ ). The analytical results reported in Table 2 show a rather good agreement between nominal and analyzed Sb concentration, while lead concentration is smaller than expected. Silicon content that arises from crucible increases as PbO concentration and melting time increase.

Table 2:

Acronym	mol %		Nominal composition			Analyzed composition			
	$\text{Sb}_2\text{O}_3$	PbO	Sb	Pb	O	Sb	Pb	O	Si
50 $\text{Sb}_2\text{O}_3$ 50PbO	50	50	28.57	17.14	57.14	29.5	13.4	55.8	1.3
40 $\text{Sb}_2\text{O}_3$ 60PbO	40	60	25	18.75	56.25	21.7	17.2	54.8	0.9
30 $\text{Sb}_2\text{O}_3$ 70PbO	30	70	20.68	24.13	48.27	21.5	22.3	52.6	3.5
20 $\text{Sb}_2\text{O}_3$ 80PbO	20	80	15.38	30.76	53.84	15.6	27.1	54.0	3.3
10 $\text{Sb}_2\text{O}_3$ 90PbO	10	90	8.69	39.13	52.17	8.2	31.8	55.6	4.4

Glass formation has been investigated in various  $\text{Sb}_2\text{O}_3$ -PbO-  $\text{Me}_2\text{O}_3$  ternary systems, where Me = Al, In, Ga. Corresponding vitreous areas in nominal compositions are reported in fig3.

For all these systems, the experimental vitreous area is very narrow. For example,  $\text{In}_2\text{O}_3$  content should not exceed 5 mol % while it may reach 15 mol % with  $\text{Al}_2\text{O}_3$  and  $\text{Ga}_2\text{O}_3$ . Sample color remains yellow for the ternary glasses containing  $\text{Al}_2\text{O}_3$  and  $\text{Ga}_2\text{O}_3$  but it turns to green for the largest  $\text{In}_2\text{O}_3$  contents.

### 3.2 X Ray Diffraction

The XRD patterns confirm the amorphous character of the samples, as shown in figure 4 for typical glass compositions. These patterns show a broad main peak at  $2\Theta = 27,9^\circ$ . Beyond this peak, a second one is observed at  $2\Theta = 54^\circ$ .

### 3.3 Thermal Properties:

#### 3.3.1 Binary system

Differential Scanning Calorimetry has been implemented between 100 and 500°C. Typical DSC scans are reported in figure 5.

The evolution of the characteristic temperatures corresponding to glass transition ( $T_g$ ), onset of crystallization ( $T_x$ ) and exotherm maximum ( $T_p$ ) versus concentration is plotted in figure 6(a) The stability factors  $S$  [19] and  $\Delta T = T_x - T_g$  [20] that give an estimate of glass forming ability appears in figure 6(b). Glass transition varies between 255 and 276°C. As one could expect, characteristic temperatures depends on  $\text{Sb}_2\text{O}_3$  content. These results suggest that glass stability against devitrification is maximum for high  $\text{Sb}_2\text{O}_3$  concentration ( $> 70\%$ ) and for

1 large lead concentration (90 % PbO). Intermediate compositions appear more prone to  
2 devitrification.  
3

### 4 **3.3.2 Ternary system**

5  
6  
7  
8 For comparison, thermal measurements have been carried out on a set of three samples with  
9 the same general, formula:  $x \text{Sb}_2\text{O}_3 - (95-x) \text{PbO} - 5\text{Me}_2\text{O}_3$  (Me = Al, Ga, In, and  $10 < x < 80$ )

10 The composition dependence of glass transition temperature ( $T_g$ ) is reported in fig 7. The  
11 curves expressed the same behavior as observed in the binary system for glass transition:  $T_g$   
12 increases for large PbO concentrations ( $> 40\%$ ). In a general way,  $T_g$  increases with ionic  
13 radius ( $\text{Al}^{3+} < \text{Ga}^{3+} < \text{In}^{3+}$ ).  
14

15 We have also prepared samples with different  $\text{In}_2\text{O}_3$  contents. The basic composition - 50  
16  $\text{Sb}_2\text{O}_3 - 50\text{PbO}$  - was chosen in the range of minimum stability in order to make clear the effect  
17 of additive concentration on glass stability. As shown in figure 8, a first result concerns  $T_g$   
18 that increases with  $\text{In}_2\text{O}_3$  concentration.  
19  
20

21 Another set of glass samples was prepared with the general formula:  $50 \text{Sb}_2\text{O}_3 - (50-x) \text{PbO} - x$   
22  $\text{Me}_2\text{O}_3$  (Me= Al, Ga, In). Glass transition  $T_g$  increases quasi-linearly with  $\text{Me}_2\text{O}_3$  addition.  
23 Once again, larger  $T_g$  values are observed for cations with larger ionic radius.  
24  
25  
26

27 Figure 10 reports the variation of the stability factor  $S$  as a function of  $\text{Me}_2\text{O}_3$  concentration  
28 for the  $50 \text{Sb}_2\text{O}_3 - (50-x) \text{PbO} - x \text{Me}_2\text{O}_3$  glasses.  
29

30 These curves suggest that  $\text{Me}_2\text{O}_3$  addition has a stabilizing effect by comparison to the binary  
31 glass. At first glance, glasses containing Ga content appear as the most stable ones. However  
32 additional experiments should be implemented to confirm these observations: first, no data  
33 were collected for  $\text{Me}_2\text{O}_3$  concentrations between 5 and 10 mol %; and second, no stable glass  
34 was obtained for  $\text{In}_2\text{O}_3$  concentrations larger than 5 mol % (see fig. 3). Then one would  
35 expect the sharp decrease of the stability factor beyond some threshold value that could be  
36 found experimentally.  
37  
38  
39  
40

### 41 **3.4 Density**

42 The composition dependence of the density of the binary glass samples in the  $\text{Sb}_2\text{O}_3 - \text{PbO}$   
43 system is shown in fig 11.  
44  
45  
46

47 As one could expect, density  $d$  decreases as lead oxide is replaced by antimony sesquioxide.  
48 This change is approximately linear. Another set of density measurement has been  
49 implemented in the ternary system with the following formula:  $x\text{Sb}_2\text{O}_3 - (95-x) \text{PbO} - 5\text{Me}_2\text{O}_3$   
50 (Me = Al, Ga, In). As shown in figure 12, density also decreases linearly with the substitution  
51 of PbO by  $\text{Sb}_2\text{O}_3$ .  
52  
53  
54

### 55 **3.5 Microhardness**

56 Figure 13 shows the microhardness variation of the  $50\text{Sb}_2\text{O}_3 - (50-x) \text{PbO} - x\text{Me}_2\text{O}_3$  (Me = Al,  
57 Ga, In) glasses as a function of  $\text{Me}_2\text{O}_3$  concentration. Microhardness increases with  $\text{Me}_2\text{O}_3$   
58  
59  
60  
61  
62  
63  
64  
65

concentration. For the same oxide content microhardness increases according to the sequence:  $H_v(\text{Al}) < H_v(\text{Ga}) < H_v(\text{In})$

## Discussion

This study exemplifies the respective parts of the glass components. Antimony sesquioxide  $\text{Sb}_2\text{O}_3$  is clearly a vitrifying oxide. Even though the existence of pure vitreous  $\text{Sb}_2\text{O}_3$  has been for long a matter of discussion, the occurrence of numerous binary glasses with high  $\text{Sb}_2\text{O}_3$  concentration confirms its glass forming ability. It complies with Zachariasen's rules[7] insofar as it forms tetrahedra in the solid state that must be written  $\text{SbO}_3(\text{LP})$ , where LP is a lone pair of  $s^2$  electrons. In this way it offers similarities with phosphate groups  $\text{PO}_4$  in which one oxygen is non-bridging. The vitreous network is constructed from these  $\text{SbO}_3(\text{LP})$  tetrahedra, with up to three non-bridging oxygens.

Lead oxide  $\text{PbO}$  is known to have a dual role, depending on glass composition and also on the nature of the other vitrifiers. Solid state chemistry teaches that  $\text{Pb}^{2+}$  commonly acts as a large cation that leads to compounds isostructural with those obtained with  $\text{Sr}^{2+}$ ,  $\text{Ba}^{2+}$  or  $\text{Eu}^{2+}$ . Among other examples one may quote perovskite  $\text{PbZrO}_3$  and fluorite-type  $\text{PbF}_2$ . In these structures, coordination number is high: 12 in perovskite and 8 in fluorite [21]. Based on this coordination and the corresponding size effect, divalent lead is considered as a modifier that fills empty space within the vitreous network. This behavior is common at low  $\text{PbO}$  content. However, at high concentrations, the structural behavior of  $\text{Pb}^{2+}$  is different and compares to that of trivalent antimony. Its coordination number drops down while a lone pair of  $s^2$  electrons completes a smaller coordination polyhedron. This polyhedron typically consists of 4 oxygens and one lone pair. This makes the basis of the  $\text{PbO}$  structure. Then this  $\text{PbO}_4$  group can enter the vitreous network. Indeed there are numerous examples of glass compositions with a very large content of lead oxide. In the  $\text{Sb}_2\text{O}_3$ - $\text{PbO}$  binary system, there are two different glass domains, the first one for large  $\text{Sb}_2\text{O}_3$  concentrations and the second one when lead is predominant. Not surprisingly characteristic temperatures reflect this situation (fig. 6): less stable glasses are found in the intermediate composition range.

The optical quality of the glass samples is very sensitive to the redox conditions. There are several redox couples that interact in glass melt:  $\text{Sb}^{3+}/\text{Sb}^{5+}$ ,  $\text{Pb}^{2+}/\text{Pb}^{4+}$ ,  $\text{Pb}^0/\text{Pb}^{2+}$ . Equilibrium constants vary with temperature. In order to limit the formation of reduced species, it is necessary to maintain an oxidizing atmosphere that can be provided by room atmosphere. However, in some cases, longer melting – and fining- time are required. When silica crucibles are used, this results in a larger contamination by silica. This drawback is avoided with other crucible materials such as alumina.

The influence of the third component on thermal properties is unexpected. In classical oxide glasses –silicates, phosphates, borates- glass transition temperature decreases as the ionic radius of the modifying element increases:  $T_g$  is smaller when sodium is replaced by potassium, rubidium or cesium. When network formers are incorporated,  $T_g$  variation is ruled by the relative bond strength of the new element. For example, the Si/Ge substitution leads to lower  $T_g$ 's. In these glasses, the bond strength of aluminum vs. oxygen is much larger than that of gallium and indium. However, for the same nominal composition, larger  $T_g$  is observed with  $\text{Ga}_2\text{O}_3$  and  $\text{In}_2\text{O}_3$  (fig. 9). Then, it appears that bond strength is not the major parameter to account for this observed variation. Rather changes in glass structure should be considered. While these three cations –Al,Ga,In- are likely to enter the vitreous network, their coordination number is expected to be 6. As a result, the number of non-bridging oxygens is reduced, and consequently, glass transition temperature is lowered. This mechanism could

also explain the increase of microhardness with the incorporation of the  $\text{Me}_2\text{O}_3$  oxides in the  $\text{Sb}_2\text{O}_3$ - $\text{PbO}$  binary glass (fig. 13).

## Conclusion

The incorporation of trivalent oxides in the  $\text{Sb}_2\text{O}_3$ - $\text{PbO}$  binary glass has been studied. Characteristic temperatures, density and microhardness have been measured for binary glasses. The limits for glass formation have been defined by a set of systematic experiments in the  $\text{Sb}_2\text{O}_3$ - $\text{PbO}$ - $\text{Me}_2\text{O}_3$  ( $\text{Me}=\text{Al}, \text{Ga}, \text{In}$ ) ternary systems. Up to 10 mol %  $\text{Me}_2\text{O}_3$  oxide could enter glass composition. Thermal measurements show that characteristic temperatures increase with oxide addition. In the mean time, glass is less prone to devitrification. Glass transition temperature increases according to the sequence:  $T_g(\text{Al}) < T_g(\text{Ga}) < T_g(\text{In})$ . Microhardness variation is similar, and maximum values are observed for indium containing glasses. It is suggested that this unexpected variation occurs from the decrease of the number of non-bridging oxygens. This decrease could result from the 6 coordination number of the trivalent cations that take place in the vitreous network.

## Acknowledgment

The authors would like to thanks PNE (Algerian program) for the financial support.

## References

- [1] J.M. Fernández Navarro, *El Vidrio. Constitución, fabricación, propiedades*, Consejo Superior de Investigaciones Científicas, Madrid, 2003.
- [2] C. Moretti, English lead crystal. The Ravenscroft recipe and points not clear on the process of development of “flint” glass formulation, Proc. of the 16<sup>th</sup> Congress of the AIHV, London, 7–13 September 2003, 2005.
- [3] W.H. Dumbaugh, J.C. Lapp, *J. Am. Ceram. Soc.* 75 (1992) 2315-2326.
- [4] J.S. Wang, E.E. Vogel, Snitzer, *Opt. Mater* 3 (1994) 187-203.
- [5] B. Dubois, H. Aomi, J.J. Videau, J. Portier, Haggemuller, *Mater.Res Bull.* 19(10) (1984) 1317-1323.
- [6] R.E.de Araujo, C.B. de Araujo, G. Poirier, M. Poulain, Y. Messaddeq, *Appl. Phys. Lett* 81(2002) 4694-4696.
- [7] W.H Zachariasen, *J.Chem. Soc* 54(1932)3841
- [8] M.T. Soltani, A. Boutarfaia, R. Makhloufi, M. Poulain, *J. Phys. Chem. Solids* 64 (2003) 2307–2312
- [9] A. Winter, *Verres Réfract.*, 36 (2), 353-356 (1982)
- [10] Y. Taibi, M. Poulain, R. Lebullenger, L. Atoui, M. Legouera, *J Opt Adv Mat.* 11 (2009) 34 - 40
- [11] K. Nageswara Rao, N. Veeraiyah, *Ind. J. Phys.* 74A (2000) 37
- [12] M.R. Reddy, S.B. Raju, N. Veeraiyah, *J. Phys. Chem. Solids* 61 (2000) 1567.
- [13] P. Kantor, A. Revcolevschi, R. Collongues, *J. Mater. Sci.* 8 (1973) 1359.
- [14] H. Morikawa, J. Jegoudez, C. Mazieres, A. Revcolevschi, *J. Non-Cryst. Solids* 44 (1981) 107.
- [15] W.H. Dumbaugh, *Phys. Chem. Glasses* 27 (1986) 119.
- [16] J.E. Shelby, *J. Am. Ceram. Soc.* 71 (1988) C-254.
- [17] F. Miyaji, K. Tadanaga, T. Yoko, S. Sakka, *J. Non-Cryst.Solids* 139 (1992) 268.
- [18] K. Suzuya, C.-K. Loong, D.L. Price, B.C. Sales, L.A. Boatner, *J. Non-Cryst.Solids* 258 (1999) 48-56.

[19] M. Saad, M. Poulain, Mat. Sci. Forum 19&20 (1987) 11.

[20] A. Dietzel, Glastech. Ber., **22**(7), 41 (1968).

[21] Yet-Ming Chiang, Dunbar Birnie III, David Kingery, Physical Ceramics- Principles for Ceramic Science and Engineering, John Wiley (1997).

1  
2  
3  
4  
5  
6  
7  
8  
9  
10  
11  
12  
13  
14  
15  
16  
17  
18  
19  
20  
21  
22  
23  
24  
25  
26  
27  
28  
29  
30  
31  
32  
33  
34  
35  
36  
37  
38  
39  
40  
41  
42  
43  
44  
45  
46  
47  
48  
49  
50  
51  
52  
53  
54  
55  
56  
57  
58  
59  
60  
61  
62  
63  
64  
65



Figures of the manuscript :

INVESTIGATION AND PROPERTIES OF NOVEL LOW MELTING GLASSES IN  
THE TERNARY SYSTEM  $Sb_2O_3$ - $PbO$ - $Me_2O_3$

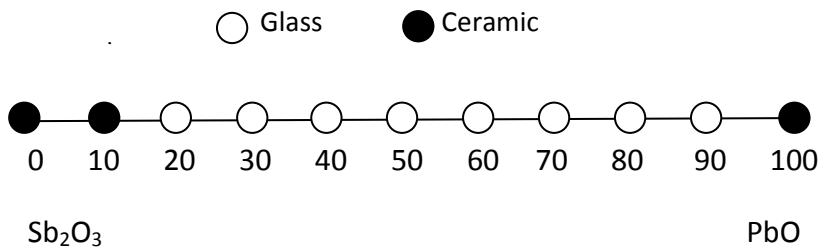


(fig 1)

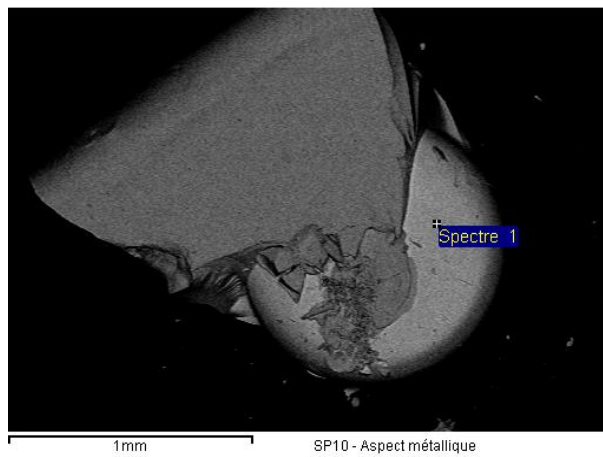
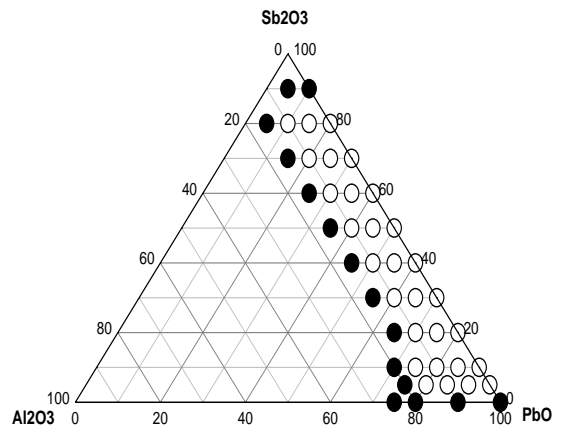
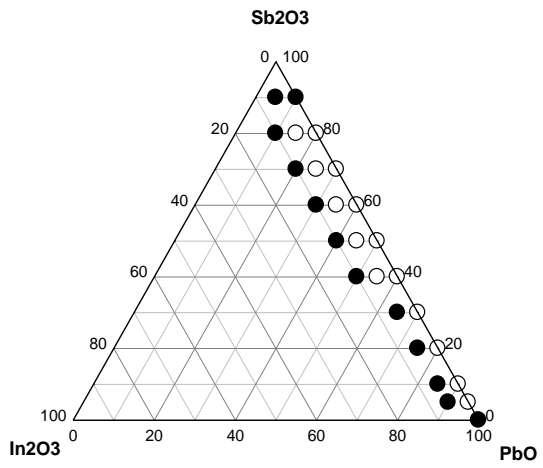
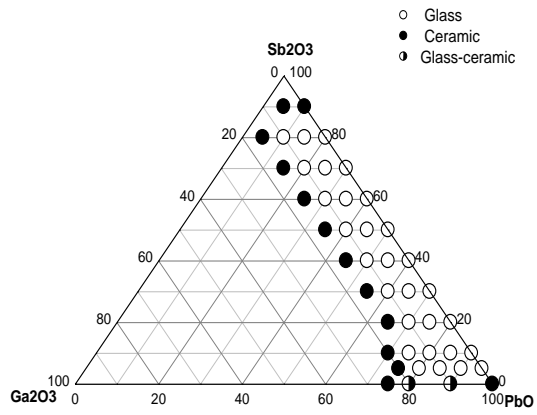


(fig 2)



These 3 diagrams belong to the same figure (figure 3)

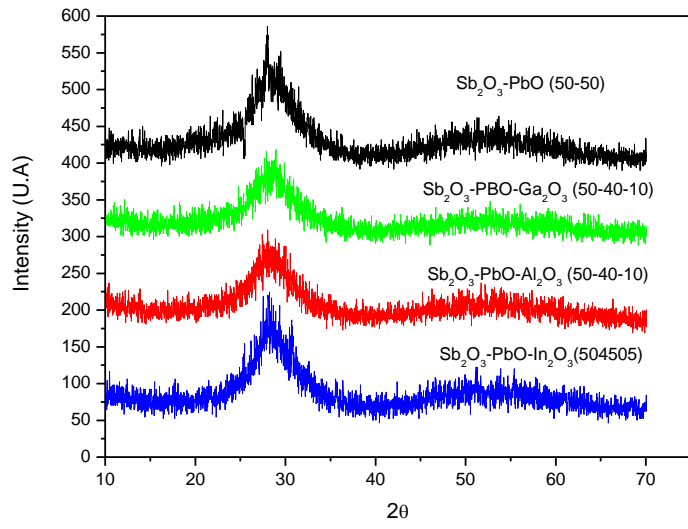


( Fig 4)

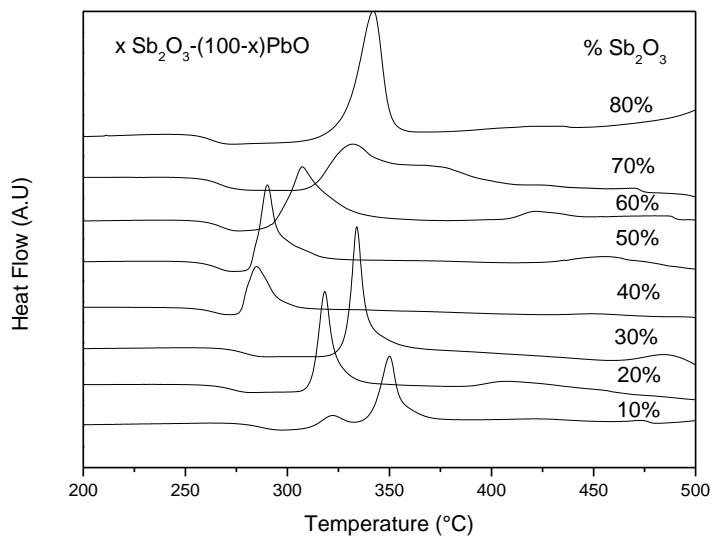


(fig 5)

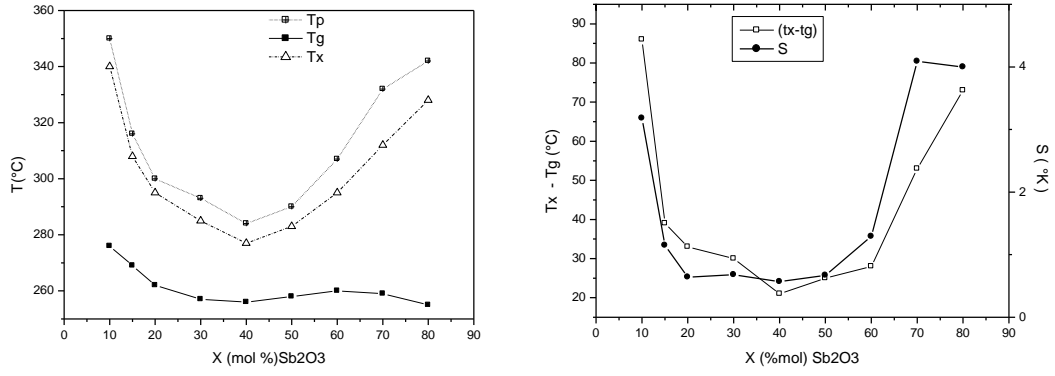


(Fig 6)

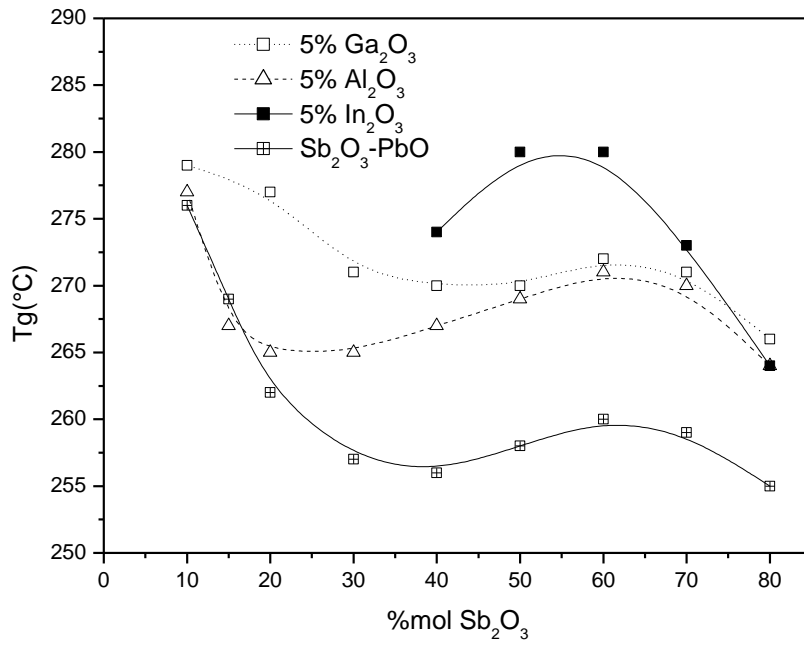


(Fig 7)

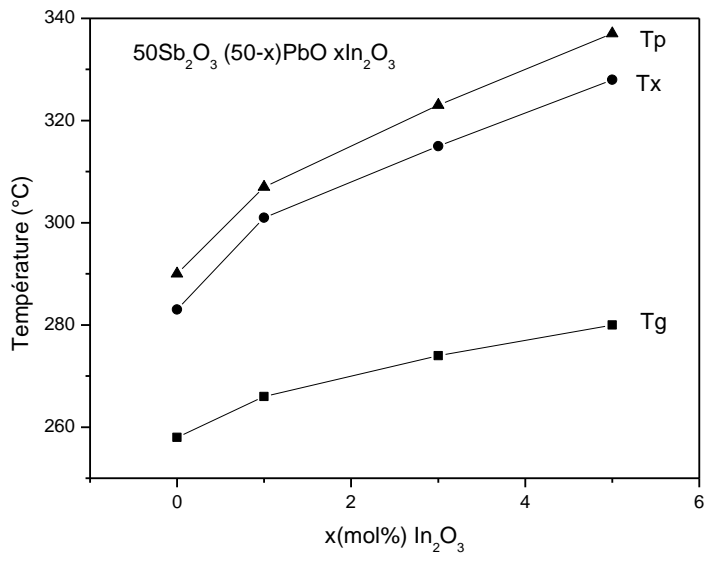


(fig 8)

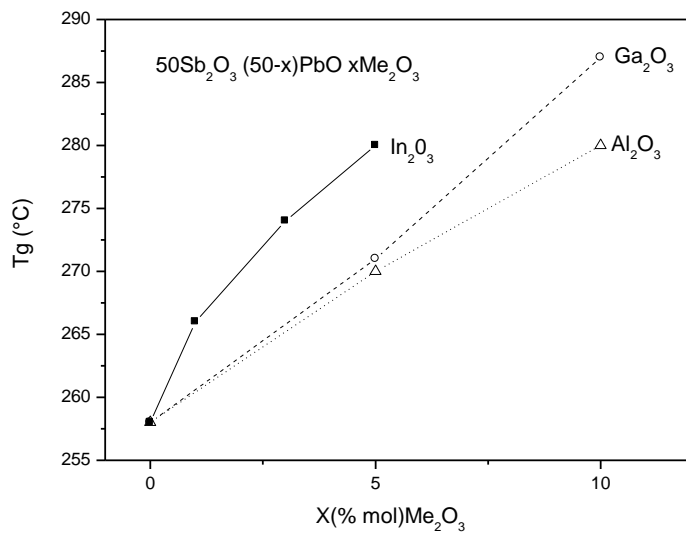


(fig 9)

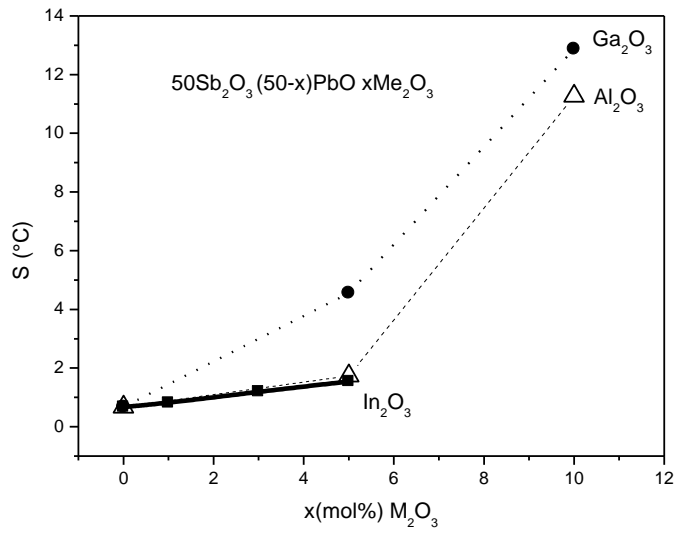


(fig 10)

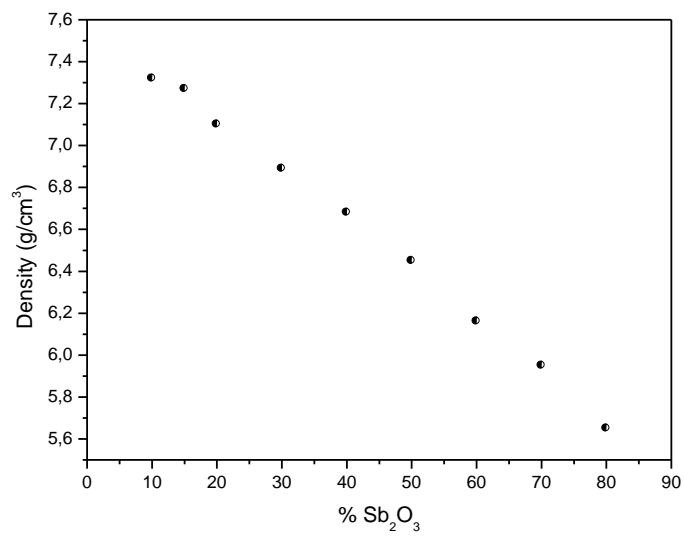


(fig 11)

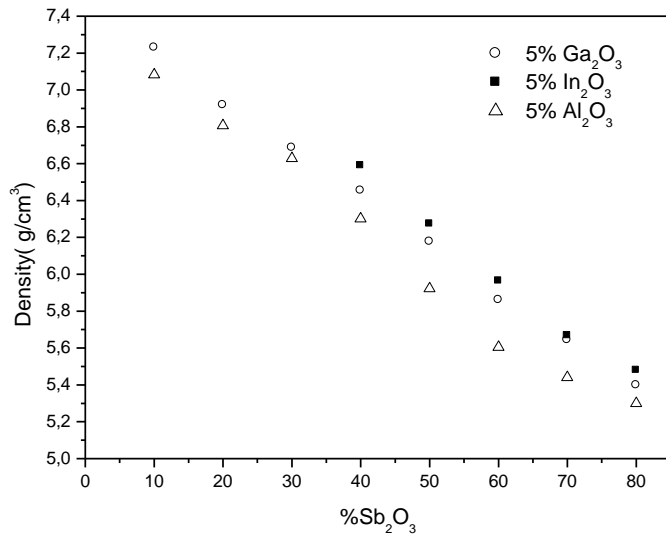


(fig 12)

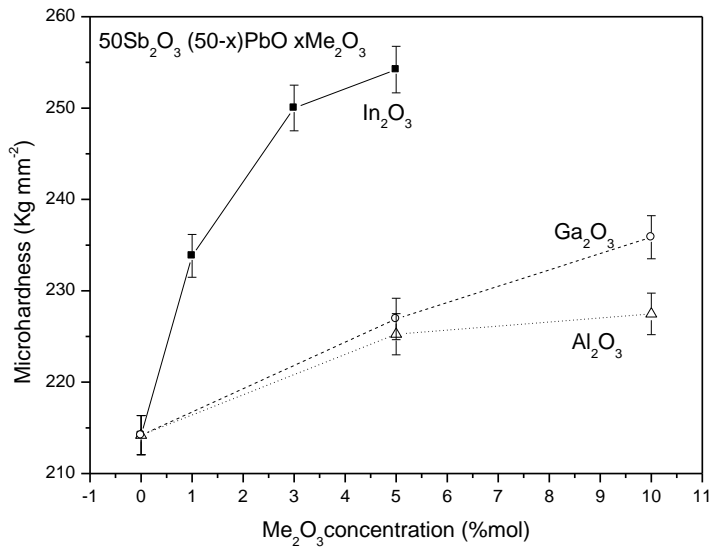


(fig 13)